Gene therapy restores vision in a canine model of childhood blindness

Gregory M. Acland[1], Gustavo D. Aguirre[1], Jharna Ray[1], Qi Zhang[1], Tomas S. Aleman[2], Artur V. Cideciyan[2], Susan E. Pearce-Kelling[1], Vibha Anand[2], Yong Zeng[2], Albert M. Maguire[2], Samuel G. Jacobson[2], William W. Hauswirth[3] & Jean Bennett[2]

The relationship between the neurosensory photoreceptors and the adjacent retinal pigment epithelium (RPE) controls not only normal retinal function, but also the pathogenesis of hereditary retinal degenerations. The molecular bases for both primary photoreceptor[1] and RPE diseases[2–4] that cause blindness have been identified. Gene therapy has been used successfully to slow degeneration in rodent models of primary photoreceptor diseases[5,6], but efficacy of gene therapy directed at photoreceptors and RPE in a large-animal model of human disease has not been reported. Here we study one of the most clinically severe retinal degenerations, Leber congenital amaurosis (LCA). LCA causes near total blindness in infancy and can result from mutations in *RPE65* (LCA, type II; MIM 180069 and 204100). A naturally occurring animal model, the *RPE65*$^{-/-}$ dog, suffers from early and severe visual impairment similar to that seen in human LCA. We used a recombinant adeno-associated virus (AAV) carrying wild-type *RPE65* (AAV-*RPE65*) to test the efficacy of gene therapy in this model. Our results indicate that visual function was restored in this large animal model of childhood blindness.

RPE65 is an evolutionarily conserved, 65-kD membrane-associated protein[7,8], involved in retinoid metabolism[9–11]. *Rpe65* deficiency in mice results in accumulation of all-*trans*-retinyl esters, undetectable levels of rhodopsin, rod photoreceptor dysfunction, inclusions in the RPE and slow retinal degeneration[12,13]. 9-*Cis*-retinal can restore visual pigment and function in *Rpe65*-deficient mice[13]. Visual impairment in *RPE65*$^{-/-}$ dogs is caused by a homozygous 4-bp deletion in *RPE65* (refs. 14,15) resulting in a frameshift and a premature stop codon, which truncates the protein. Histopathology in homozygous dogs shows prominent RPE inclusions and slightly abnormal rod photoreceptor morphology early in life[14,15], and slowly progressive photoreceptor degeneration[14].

We cultured RPE cells from eyes of a wild-type and an affected dog, and infected the *RPE65*$^{-/-}$ cells with AAV-*RPE65*. As shown by immunohistochemistry (Fig. 1*a*), wild-type RPE cells possessed high levels of RPE65. In contrast, RPE65 was absent from untreated, mutant RPE cells (Fig. 1*b*). After infection with AAV-*RPE65*, mutant RPE cells labeled positively for RPE65 (Fig. 1*c*). We observed complementary immunohistochemical results in sections from untreated wild-type versus *RPE65*$^{-/-}$ retinas (Fig. 1*d*,*e*).

We confirmed infection of the mutant RPE cells by AAV-*RPE65* and subsequent expression of the wild-type *RPE65* transgene using PCR amplification and western-blot analysis, respectively. We used PCR to amplify the wild-type *RPE65* DNA fragment (109 bp) in transduced RPE cells (Fig. 2*a*, lane 12). Non-transduced RPE from the same animal yielded only mutant DNA (105 bp). RPE65 protein in transduced cells was detected by western-blot analysis (Fig. 2*c*, lane 12).

We delivered AAV-*RPE65* intra-ocularly to three *RPE65*$^{-/-}$ dogs (Table 1) and assessed the consequences by electroretinography[16] (ERG; Fig. 3). The ERG of the normal dog (Fig. 3*a*, left) responded to increasing stimulus intensity with increased bipolar cell (b-wave) and photoreceptor (a-wave) amplitudes. Compared with normal dogs, the threshold stimulus required to elicit an ERG response from 4-month *RPE65*$^{-/-}$ dogs was elevated by over 4.5 log units (Fig. 3*a*, middle). Higher-energy stimuli and recording criteria that elicit, in normal dogs, saturated ERG photoresponses originating from photoreceptors (Fig. 3*b*, left) yielded no detectable signals in affected animals (Fig. 3*b*, middle). A cone-isolated flicker ERG response (Fig. 3*c*, left) was absent from affected animals (Fig. 3*c*, middle).

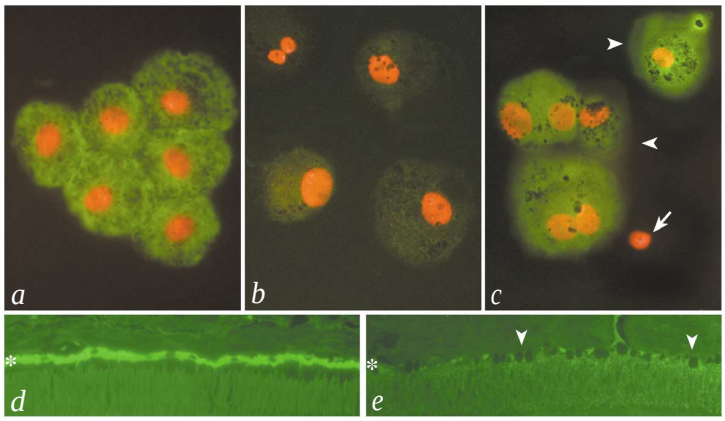

Fig. 1 RPE65 immunocytochemistry in canine RPE cells and retinal sections. Shown are cultured canine RPE cells immunolabeled with anti-RPE65 antibody, with nuclei stained with propidium iodide. ***a***, Wild-type cells label uniformly and intensely with anti-RPE65 antibody. ***b***, *RPE65*$^{-/-}$ cells, 60 d in culture, before infection with AAV-*RPE65* do not label. ***c***, *RPE65*$^{-/-}$ cells, 60 d in culture, 10 d post-infection with AAV-*RPE65*. Most cells (arrowheads) label positively, indicating presence of wild-type RPE65 protein. One cell (arrow) does not seem to have been transduced. ***d***, Wild-type retina. The RPE (*) is distinctly and uniformly labeled. ***e***, *RPE65*$^{-/-}$ retina. The RPE (*) shows only background autofluorescence. Arrowheads indicate lipid inclusions in diseased RPE cells.

[1]*James A. Baker Institute for Animal Health, College of Veterinary Medicine, Cornell University, Ithaca, New York, USA.* [2]*F.M. Kirby Center, Scheie Eye Institute and Department of Ophthalmology, University of Pennsylvania, Philadelphia, Pennsylvania, USA.* [3]*Department of Ophthalmology and Powell Gene Therapy Center, University of Florida, Gainesville, Florida, USA. Correspondence should be addressed to J.B. (e-mail: jebennet@mail.med.upenn.edu).*

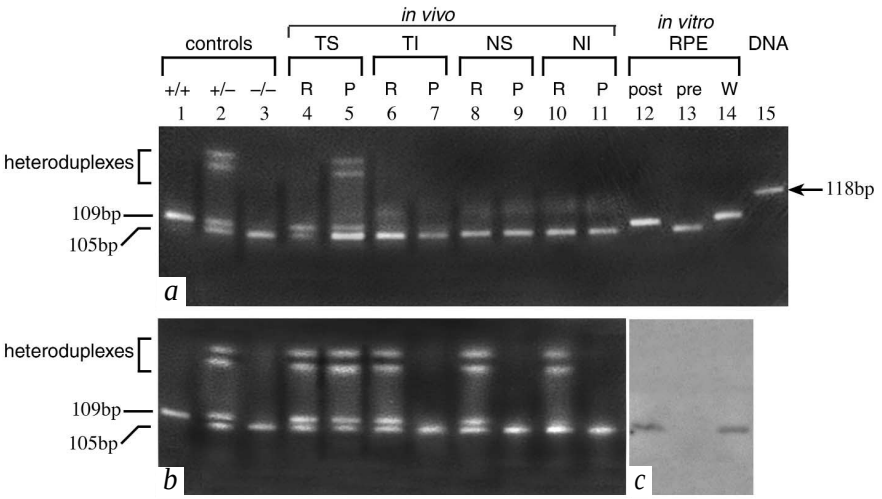

Fig. 2 Persistence and expression of the *RPE65* transgene after *in vivo* delivery to neural retina (R) and RPE/choroid (P), and after *in vitro* delivery to RPE cells (RPE). Amplification of the region spanning the canine *RPE65* mutation results in either a wild-type (endogenous or virally delivered) product (109 bp) or a mutant product (105 bp). Lanes 1–3 of both (***a***) and (***b***) show results of genomic PCR from homozygous wild-type (+/+), heterozygous (+/–) and homozygous mutant ('affected'; *RPE65*$^{-/-}$) controls. Where both products amplify, additional bands representing heteroduplexes are also seen. Samples from one (affected) dog eye treated *in vivo* (right eye of BR29; lanes 4–11) were used for genomic PCR (*a*) and RT–PCR (*b*). Samples from affected RPE, cultured *in vitro*, were also evaluated for presence of wild-type and/or mutant *RPE65* (lanes 12–14). Results of western-blot analysis of treated and untreated RPE cells are shown in (***c***). ***a***, Genomic PCR demonstrates persistence of viral DNA in neural retina and RPE-choroid treated *in vivo* from temporal-superior (TS, injected) quadrant (lanes 4, 5), but in other quadrants (TI, temporal-inferior; NS, nasal-superior; NI, nasal-inferior; lanes 6–11) amplification product is below detectable levels. *In vitro* assays show that, in uninfected cultured RPE from a mutant dog ('pre', lane 13), only the mutant product was amplified. Ten days post-transfection, however, the normal transgene yielded the overwhelming product ('post', lane 12). Results are similar to those found using cultured RPE from a wild-type dog ('W', lane 14). DNA, (unamplified) ϕX174 DNA digested with *Hae*III. ***b***, RT–PCR (lanes 4–11) demonstrates expression of wild-type message in neural retina (R) treated *in vivo* from all four quadrants (lanes 4, 6, 8 and 10), but in RPE-choroid (P), from the injected quadrant only (lane 5). Lanes 1–3, genomic PCR controls. ***c***, Western-blot analysis demonstrates absence of RPE65 protein from mutant RPE cells before transfection (lane 13), but presence of the protein afterwards (lane 12). Proteins were labeled with anti-RPE65 antibody. Lane 12, 10 d post-infection with AAV-*RPE65* (83 μg); lane 13, before infection (104 μg); lane 14, wild-type control (160 μg).

Retinal function was improved in eyes treated with subretinal AAV-*RPE65* (Fig. 3*a–c*, right) compared with the same eyes before treatment (Fig. 3*a–c*, middle). Responses from the right eye of BR33 (Fig. 3*a*, right) had b-wave thresholds lower by approximately 4 log units than pre-treatment and were similar to normal (Fig. 3*a*, left). ERG photoresponses in 3 subretinally injected eyes showed maximal amplitudes of 27, 36 and 58 μV (Fig. 3*b*, right), representing approximately 16% of normal amplitudes (Fig. 3*b*, left; mean±s.d.=246±95 μV; n=7). Photoresponse amplitudes in these eyes were significantly different ($P<0.05$) from the amplitudes in untreated eyes (Fig. 3*b*, middle; 14±3.4 μV; n=3). Cone flicker ERGs were recordable post-treatment (Fig. 3*c*, right); amplitudes ranged from 4 to 6 μV (Fig. 3*c*, right), representing approximately 16% of normal (Fig. 3*c*, left; 30±8 μV). Intravitreally injected eyes showed no difference from untreated eyes for all ERG parameters.

We demonstrated transmission of retinal activity to higher visual pathways by pupillometry. At a suprathreshold intensity (Fig. 3*d*), pupillary constriction was greatest in normal dogs and least in untreated *RPE65*$^{-/-}$ dogs. The subretinally treated eye of BR33 responded midway between normal and untreated (Fig. 3*d*). The threshold intensity to reach a criterion pupillary response (Fig. 3*e*) was improved in subretinally treated compared with untreated eyes. Consistent with ERG and pupillometry results, flash-evoked visual cortical potentials in the dark-adapted state yielded waveforms from the subretinally (but not intravitreally) treated eye (data not shown).

We performed qualitative visual assessment of the three treated animals at four months after injection. Results of behavioral testing were consistent with the electrophysiological results. For example, dog BR33 was consistently (5/5 observers) scored as 'normally sighted' under photopic (room lighting) conditions. Under dim red light, this dog consistently avoided objects directly in front and on the right (the side injected subretinally), but consistently failed to avoid objects on the left (injected intravitreally; $P=0.0048$). In contrast, the untreated affected dog, BR46, did not display avoidance behavior in any direction (Web Fig.A and Web Movie).

To correlate transgene expression with changed visual function, we surgically enucleated one subretinally injected eye 99 days after injection, and harvested retinal and RPE/choroid tissues. Persistence of transferred DNA, evaluated by genomic PCR, was restricted to the injected quadrant (Fig. 2*a*). RPE/choroid from this quadrant (Fig. 2*b*, lane 5) expressed a higher ratio of wild-type to mutant *RPE65* than that from other quadrants. Neural retina also expressed the transgene, with highest levels present in the injected quadrant.

This proof-of-concept study is the first to show that gene therapy can restore vision in a large-animal model of a human retinopathy. Although previous

Table 1 • Procedures performed on the eyes of four dogs with mutant *RPE65*

Animal	Age at day 0	Eye	Injection route	Dose	Vol	ERG age	Rescue effect
BR29	132	R	SR	3.7	150	227	+
		L	NI	–	–	227	–
BR33	124	R	SR	4.6	200	219	+
		L	IV	4.6	200	219	–
BR47	108	R	SR	4.6	200	203	+
		L	IV	4.6	200	203	–
BR46	108	R	NI	–	–	203	–
		L	NI	–	–	203	–

Age, days postnatal; R, right eye; L, left eye; SR, subretinal injection; IV, intravitreal injection; NI, not injected; dose×10^{10}, infectious particles AAV-*RPE65* injected; Vol, volume injected, in microliters. Baseline ERGs were recorded two weeks before injection. For rescue effect (assessed by ERGs recorded 95 d after injection): +, positive effect; –, no effect apparent.

studies have demonstrated that gene therapy can delay retinal degeneration, here we have demonstrated definitive recovery of function. In addition, small-animal studies have shown histologic and electrophysiologic correlates of visual function to be partially preserved, but this large-animal study shows the presence of vision with regard to both psychophysical and behavioral measures. Therapeutic effect required delivery of wild-type *RPE65* to the outer retina. Function was not restored after intravitreal injection of vector, a route that targets ganglion cells (but not RPE/photoreceptors) efficiently[17]. Although the vector used here transduces photoreceptors and other retinal neurons, it is likely that it is expression of the wild-type transgene in RPE cells (and not photoreceptors) that rescues the mutant phenotype. The RPE alone possesses the components necessary to supply chromophore to rod photoreceptors, although there may be a retinal retinoid metabolism for cones (not involving RPE65; ref. 12)

A logical question leading from our results is whether subretinal injection of AAV-*RPE65* would also correct the functional defects found in humans with LCA due to *RPE65* mutations. Currently, there is no treatment for LCA and related early onset retinal degenerative diseases. If long-term preservation of structure despite loss of function is a feature of RPE-associated retinopathy[13], delivery of *RPE65* to defective RPE cells could conceivably restore some functional vision to humans as well. Additional long-term safety and efficacy studies must be performed before initiating such trials.

Note: supplementary information is available on the Nature Genetics web site (http://genetics.nature.com/supplementary_info/).

Methods

Virus preparation. Recombinant AAV vector was based on pTR-UF2, in which the 472-bp mouse *Rho* promoter drives expression of green fluorescent protein[18] (*GFP*). For AAV-*RPE65*, the opsin promoter in pTR-UF2 was replaced with a CMV immediate early enhancer (381 bp)/chicken β-actin (CβA) promoter-exon 1-intron 1 (1,352 bp) element followed by a poliovirus internal ribosome entry sequence (637 bp). The latter supports expression in photoreceptors, RPE and ganglion cells (J. Li and W.W.H., unpublished data). *GFP* was replaced with the dog *RPE65* cDNA (ref. 15) by means of flanking

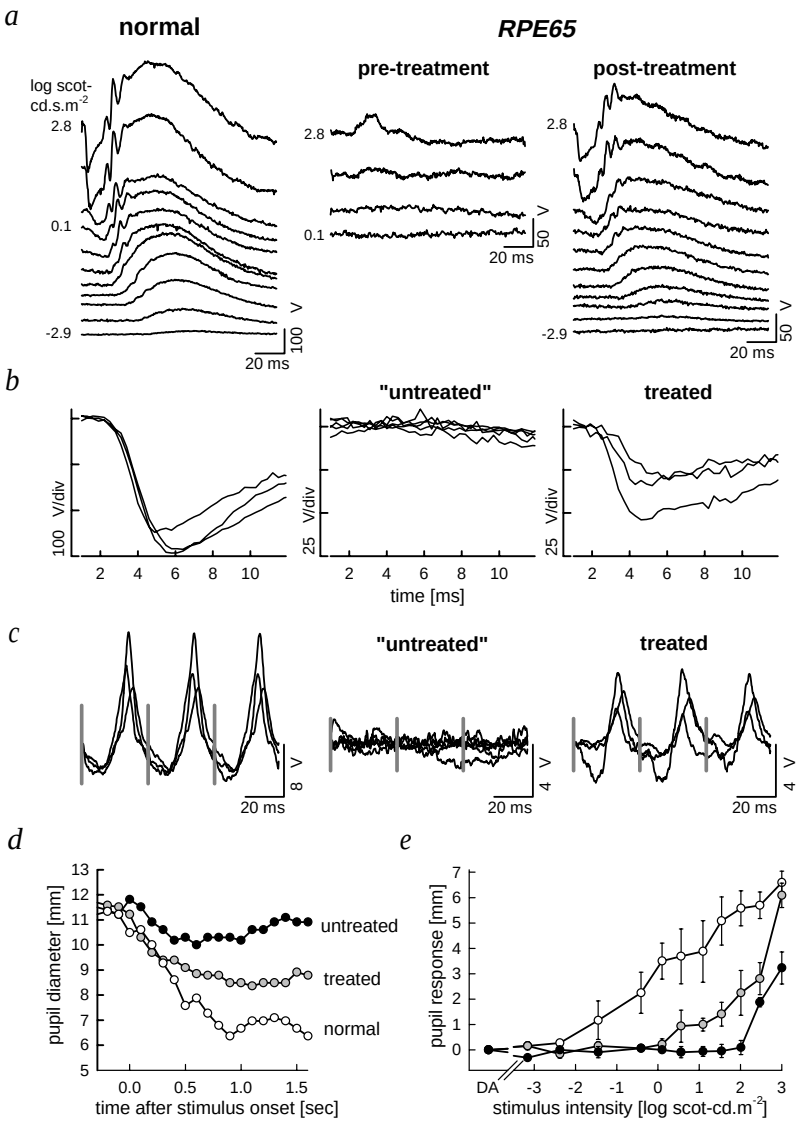

Fig. 3 Restoration of retinal and visual function in RPE65 mutant dogs by subretinal AAV-*RPE65*. ***a***, Comparison of dark-adapted ERGs evoked by increasing intensities of blue light stimuli in a control dog (left) with ERGs with the same stimuli in *RPE65* mutant dog BR33 (middle). The affected animal has elevated thresholds, reduced amplitudes and waveform shape changes (b-waves but no detectable a-waves). After subretinal AAV-*RPE65* therapy (right), the mutant dog shows an improved b-wave threshold, a large increase of a- and b-wave amplitudes (although not to normal levels), and an ERG waveform shape that is now similar to that of controls. Traces start at stimulus onset; stimulus luminance is to the left of key traces. ***b***, Details of photoreceptor function were analyzed by the amplitude and timing of the ERG photoresponses evoked by 2.8 log scot-cd.s.m^{-2} flashes; recordings from 3 control dogs (left) show ~250 μV saturated amplitudes peaking between 4.5 and 6 ms. Photoreceptor function was near noise level in three untreated eyes of *RPE65* mutant dogs and two eyes treated with intravitreal AAV-*RPE65* (middle). Photoresponses (of reduced amplitude but normal timing) were present in all three eyes that received subretinal AAV-*RPE65* (right). ***c***, Flicker ERGs in the same eyes as in (*b*) demonstrate a lack of detectable cone-mediated responses from *RPE65* mutant dogs with untreated or intravitreally treated eyes (middle). All eyes with subretinal AAV-*RPE65* treatment recovered cone flicker responses (right). Vertical gray bars denote stimulus onset. ***d***, Change in pupil diameter in response to 2.5 log cd.m^{-2} green stimulus in one eye of three representative dogs: untreated (BR46), subretinal AAV treated (BR33) and a normal control. ***e***, Pupil response as a function of stimulus intensity showed 3.8 log unit elevation of threshold (1 mm response criterion) in untreated eyes (black symbols; n=3; two eyes of BR46 and one eye of BR29) compared with normal eyes (white symbols; n=3). Eyes treated with subretinal AAV (gray symbols; n=2; BR33 and BR47) had 0.8 log unit lower thresholds compared with untreated eyes. Error bars denote s.e.m.

*Not*I sites, and the orientation and reading frame confirmed by DNA sequence analysis. Plasmid DNA containing this construct was packaged into AAV particles using iodixanol gradient purification followed by heparin-Sepharose agarose column chromatography[19]. We determined vector titers using an infectious center assay. Four AAV-*RPE65* virus preparations were made and combined to a total volume of 1.05 ml at 2.3×10^{11} infectious particles/ml. Contaminating helper adenovirus and wild-type AAV, assayed by serial dilution cytopathic effect or infectious center assay, respectively, were less than six orders of magnitude lower than vector AAV.

RPE cell culture, viral infection and surgical delivery. RPE cells were dissociated with 0.25% trypsin and plated at $1–2\times10^5$ cells/9-mm plastic dish. We infected confluent RPE cultures at 80% confluency with 2.3×10^7 AAV-*RPE65* viral particles for 4 h. For *in vivo* studies, virus was delivered subretinally or intravitreally under direct surgical visualization using described methods[20]. Each subretinal injection of vector (150–200 µl) created a retinal detachment elevating approximately 35% of the total retinal area. These detachments resolved spontaneously within 24 h. Humoral and intraocular antibodies specific to AAV capsid proteins were evaluated as described[20]. Animals were evaluated post-operatively for evidence of ocular or systemic toxicity, virus exposure to extraocular tissue, virus shedding, unfavorable immune response or other untoward effects; none was found.

Transgene persistence and transgene expression. PCR amplification used RPE65-1 (forward) and RPE65-3 (reverse) primers flanking the *RPE65* mutant deletion site[15]. PCR conditions were 94 ºC for 30 s, 60 ºC for 30 s and 72 ºC for 1 min, for 34 cycles. PCR products were separated on a 6% polyacrylamide gel. AAV-*RPE65* was used as positive control. This protocol was also used for PCR screening for shedding virus.

For expression studies, we divided the eyecup of the right eye of BR29 into temporal-superior, temporal-inferior, nasal-superior and nasal-inferior quadrants. From each quadrant, the retina and the pooled RPE/choroid were separately dissected under RNase-free conditions and rapidly frozen. Total RNA was prepared from retina and RPE/choroid using the TRIzol Reagent kit (Life Technologies). DNA was extracted from the same tissues according to the manufacturer's protocol. cDNA was amplified from total RNA using RNA PCR kit (Perkin Elmer) and the conditions listed above.

For protein studies, we evaluated RPE cells by immunocytochemistry using a rabbit anti-RPE65 peptide polyclonal antibody (provided by T.M. Redmond). For western-blot analysis, proteins from cultured RPE were electrophoresed on 12.5% SDS-polyacrylamide gel and then electrotransferred to a nitrocellulose membrane. We carried out immunodetection using the anti-RPE65 antibody followed by goat anti-rabbit secondary antibody and 125I-protein A.

ERGs. Dogs were dark-adapted (overnight), premedicated with acepromazine (0.55 mg/kg, IM) and atropine (0.03 mg/kg, IM), and anesthetized by intermittent ketamine (15 mg/kg, IV, repeated every 15 min). Pulse rate, oxygen saturation and temperature were monitored throughout. The cornea was anesthetized with topical proparacaine HCl (1%) and pupils dilated with cyclopentolate (1%) and phenylephrine (2.5%). Full-field ERGs were recorded using a computer-based system (EPIC-XL, LKC Technologies) and Burian-Allen contact lens electrodes[16] (Hansen Ophthalmics). Dark-adapted luminance-response functions were obtained with blue (Wratten 47A) flash stimuli spanning ~6 log units (–2.9 to +2.8 log scot-cd.s.m^{-2} (scotopic-candela.seconds.m^{-2})). ERG b-wave amplitudes were measured conventionally from baseline or a-wave trough to positive peak; a-wave amplitude was measured from baseline to negative peak at the maximal stimulus. For isolating cone pathway function, dogs were light-adapted and 29 Hz flicker ERGs evoked with white flash stimuli (0.4 log cd.s.m^{-2}) on a background (0.8 log cd.m^{-2}); amplitudes were measured between successive negative and positive peaks and timing from stimulus to the next positive peak. Ocular axial length and pupil diameter were measured for each experiment to permit calculation of retinal illuminance. For VECPs, dogs were exposed at 104 days post-treatment to a series of increasing intensities of blue light (Wratten 47) in the dark-adapted state.

Pupillometry. Dogs were dark-adapted for more than 3 h and pupil responses were obtained sequentially from each eye using full-field green stimuli (–3.2 to +3.0 log scot-cd.m^{-2}) of ~2 s duration. Pupils were imaged with a video camera under infrared illumination and continuously recorded on a VCR. Dynamic changes in pupil diameters were measured from single frames displayed on the video monitor in relation to the timing of each stimulus. Pupil responses were calculated by subtracting the smallest pupil diameter achieved within 2 s after the stimulus onset from the diameter measured in the dark.

Behavioral studies. We recorded ambulation of experimental and control *RPE65*$^{-/-}$ dogs through an obstacle course in dim light with an Optura Pi DV camcorder after the animals had acclimated for 20 min. Four separate observers were masked to the experimental design. The number of collisions to both the left and the right were tabulated from the recording over a series of 10 consecutive 30-s intervals. Statistical analyses were performed assuming that the probability of collisions was equal on the left and on the right using the exact test for proportion based on the binomial distribution.

Acknowledgments

We thank G. Antonini, D. Beliaav, N. Bennett, V. Chiodo, A. Nickle, V. Rininger and V. Scarpino for technical assistance, and M. Maguire for statistical advice. Support from NIH grants EY10820, EY11123, NS36202, EY06855, EY11142 and EY13132, The Foundation Fighting Blindness, Research to Prevent Blindness, T.L. Andresen Endowment, the Macular Vision Research Foundation, the LIFE Foundation, the Steinbach Foundation, the Mackall Foundation Trust and the F.M. Kirby Foundation.

Received 8 February; accepted 29 March 2001.

1. Phelan, J. & Bok, D. A brief review of retinitis pigmentosa and the identified retinitis pigmentosa genes. *Mol. Vis.* **6**, 116–124 (2000).
2. Gu, S.-M. *et al.* Mutations in *RPE65* cause autosomal recessive childhood-onset severe retinal dystrophy. *Nature Genet.* **17**, 194–197 (1997).
3. Marlhens, F. *et al.* Mutations in RPE65 cause Leber's congenital amaurosis. *Nature Genet.* **17**, 139–141 (1997).
4. Petrukin, K. *et al.* Identification of the gene responsible for Best macular dystrophy. *Nature Genet.* **19**, 241–247 (1998).
5. Hauswirth, W. & Beaufrer, L. Ocular gene therapy: quo vadis? *Invest. Ophthalmol. Vis. Sci.* **41**, 2821–2826 (2000).
6. Bennett, J. & Maguire, A. Gene therapy for ocular disease. *Mol. Ther.* **1**, 501–505 (2000).
7. Redmond, T. & Hamel, C. Genetic analysis of RPE65: from human disease to mouse model. *Methods Enzymol.* **317**, 705–724 (2000).
8. Bavik, C., Busch, C. & Eriksson, U. Characterization of a plasma retinol-binding protein membrane-receptor expressed in the retinal pigment epithelium. *J. Biol. Chem.* **267**, 23035–23042 (1992).
9. Saari, J. Biochemistry of visual pigment regeneration. *Invest. Ophthalmol. Vis. Sci.* **41**, 337–348 (2000).
10. Ma, J.-X., Xu, L., Othersen, D., Redmond, T. & Crouch, R. Cloning and localization of RPE65 mRNA in salamander cone photoreceptor cells. *J. Biol. Chem.* **1443**, 255–261 (1998).
11. Simon, A., Hellman, U., Wernstedt, C. & Eriksson, U. The retinal-pigment epithelial-specific 11-*cis* retinol dehydrogenase belongs to the family of short-chain alcohol dehydrogenases. *J. Biol. Chem.* **270**, 1107–1112 (1995).
12. Redmond, T. *et al.* RPE65 is necessary for production of 11-*cis*-vitamin A in the retinal visual cycle. *Nature Genet.* **20**, 344–351 (1998).
13. Van Hooser, J.P. *et al.* Rapid restoration of visual pigment and function with oral retinoid in a mouse model of childhood blindness. *Proc. Natl. Acad. Sci. USA* **97**, 8623–8628 (2000).
14. Wrigstad, A. Hereditary dystrophy of the retina and the retinal pigment epithelium in a strain of Briard dogs: a clinical, morphological and electrophysiological study. *Linkoping University Medical Dissertations* (1994).
15. Aguirre, G. *et al.* Congenital stationary night blindness in the dog: common mutation in the RPE65 gene indicates founder effect. *Mol. Vis.* **4**, 23 (1998).
16. Banin, E. *et al.* Retinal rod photoreceptor-specific gene mutation perturbs cone pathway development. *Neuron* **23**, 549–557 (1999).
17. Dudus, L. *et al.* Persistent transgene product in retina, optic nerve and brain after intraocular injection of rAAV. *Vision Res.* **39**, 2545–2554 (1999).
18. Flannery, J. *et al.* Efficient photoreceptor-targeted gene expression *in vivo* by recombinant adeno-associated virus. *Proc. Natl. Acad. Sci. USA* **94**, 6916–6921 (1997).
19. Hauswirth, W.W., Lewin, A.S., Zolotukhin, S. & Muzyczka, N. Production and purification of recombinant adeno-associated virus. *Methods Enzymol.* **316**, 743–761 (2000).
20. Bennett, J. *et al.* Recombinant adeno-associated virus-mediated gene transfer to the monkey retina. *Proc. Natl. Acad. Sci. USA* **96**, 9920–9925 (1999).